BEHAVIOR OF A THIN FLEXIBLE TWISTED WEB

By

Jerry L. Brown
Essex systems
U.S.A.

ABSTRACT

In an earlier IWEB paper, "A New Method for Analyzing the Deformation and Lateral Translation of a Moving Web"[5], a nonlinear PDE model, suitable for use with low-cost FEA software, was developed. That work considered only in-plane deformation of a flat web. For a twisted web, something more is needed. Attempts to run a straightforward three-dimensional model on a 3D version of the FEA software were unsuccessful. It seems that adding an extremely thin third dimension causes serious convergence difficulties for the solver. Furthermore, the number of nodes increases dramatically, causing run times to increase from minutes to hours. More sophisticated or special-purpose FEA codes might be able to cope with the problems. However, one of the goals of this work is to develop methods that will run fast on low-cost software. So, attention is focused on creating a two-dimensional solution based on concepts similar to those used in large-deflection plate theory.

This paper describes such a model. It incorporates the following features.

1. It allows analysis of the effects of rollers that have both in-plane and out-of-plane misalignment, including large rotations.
2. Since the equations of equilibrium for the in-plane stresses are the same as those used in the [5], this model is a natural extension of that work.
3. It incorporates the normal entry and normal strain boundary conditions for the downstream roller and can, therefore, include the effects of nonuniform webs and rollers.
4. Nonlinear definitions of stress and strain incorporate the effects of large rotations.

NOMENCLATURE

E	Modulus of elasticity, Pa
D	Flexural rigidity, N-m
h	Web thickness, m
L	Length of span, m
u	Particle displacement in x direction, m
u_x	Derivative of u with respect to x
u_y	Derivative of u with respect to y
v	Particle displacement in y direction, m
v_y	Derivative of v with respect to y
v_x	Derivative of v with respect to x
w	Particle displacement in z direction, m
w_x	Derivative of w with respect to x
w_y	Derivative of w with respect to y
V_u	Surface velocity of upstream roller, m/s
V_d	Surface velocity of downstream roller, m/s
ε_{xy}	Shear strain referred to deformed coordinate system
ε_{xx}	Strain in direction of deformed x-axis
ε_{yy}	Strain in direction of deformed y-axis
ε_{xo}	Machine direction strain at entry of upstream roller
μ	Poisson's ratio
σ_{yy}	Stress in direction of deformed y-axis, Pa
σ_{xx}	Stress in direction of deformed x-axis, Pa
σ_{xy}	Shear stress referred to deformed coordinate system, Pa
σ_{cr}	Critical buckling stress of a cylinder, Pa
σ_{yG}	CD compressive stress predicted by G-S model, Pa
σ_{yF}	CD compressive stress predicted by FEA model, Pa
ϕ_{cr}	Experimental value of angle at which twisted web develops wrinkle, degrees
ψ	Angle of tangent to particle trajectory of web (in relation to x-axis), radians
ρ_o	Density of relaxed web, Kg/m^3
i_1	Unit vector in direction of fiber that was parallel to x-axis before deformation
i_2	Unit vector in direction of fiber that was parallel to y-axis before deformation
i_3	Unit vector in direction of fiber that was parallel to z-axis before deformation

Subscripts

u	Upstream
d	Downstream

INTRODUCTION

An ideal model for a twisted web would include bending behavior so that wrinkling can be analyzed. Theodore von Karman developed a promising candidate. It is two-dimensional and incorporates out-of-plane displacements as well as bending.

$$\frac{\partial \sigma_x}{\partial x} + \frac{\partial \sigma_{xy}}{\partial y} = 0 \qquad (1) \qquad\qquad \frac{\partial \sigma_{xy}}{\partial x} + \frac{\partial \sigma_y}{\partial y} = 0 \qquad (2)$$

$$\left(\frac{\partial^4 w}{\partial x^4}+2\frac{\partial^4 w}{\partial x^2\partial y^2}+\frac{\partial^4 w}{\partial y^2}\right)\frac{D}{h}=\sigma_x\frac{\partial^2 w}{\partial x^2}+\sigma_y\frac{\partial^2 w}{\partial y^2}+\sigma_{xy}\frac{\partial^2 w}{\partial x\partial y} \quad (3)$$

In these equations, w is the out-of-plane displacement in the z direction; σ_x , σ_y and σ_{xy} are the in-plane stresses, D is the flexural rigidity and h is thickness. The machine direction will be assumed to be aligned with the x-axis throughout this paper. Note that there is no differentiation relative to the z-axis. Relations (1) and (2) are the plane stress equilibrium equations. The left side of (3) is the familiar thin plate equation. The right side of (3) accounts for interaction of the mid-plane stresses and bending. If these equations are modified to incorporate nonlinear finite deformation theory, it becomes theoretically possible to accurately model large angles of twist, detect the onset of instability and then analyze the web in its buckled state. Unfortunately, the fourth order terms of these equations present almost as much difficulty as a full three-dimensional treatment. This is especially true when they are extended to large rotations using finite deformation theory.

The problem becomes much easier if the model is required to work only up to the point of elastic instability. Most webs are so thin and flexible that they can be treated as membranes with no resistance to bending. This is true even when the web is twisted. Curvatures due to twisting are small and the bending moments are insignificant. It is only with the onset of buckling that large curvatures can develop in the form of narrow troughs. Therefore, the problem can be separated into two parts – unbuckled and buckled.

This model treats the unbuckled twisted web.

EARLIER WORK

Good and Straughan[1] analyzed a twisted web by assuming that each fiber in the machine direction (MD) follows a straight path between the rollers. Based on this, the MD elongation at each cross web location was estimated as a function of the twist angle and from that estimate an MD stress profile was created. This profile was then applied to an ingenious Airy's function model of a flat membrane to estimate the CD stress. Using Timoshenko's theory of buckling of a cylindrical shell, they then predicted the angle of twist necessary to cause the onset of wrinkling and found good agreement with experiments. Their method circumvents the complications of analyzing a twisted geometry. However, it does not permit accounting for the effects of the normal entry and normal strain rules at the downstream roller and, as will be seen from this analysis, these have a significant effect near the downstream roller.

Mockensturm[2] used fully nonlinear plate theory to analyze a twisted web. His method draws heavily on relatively recent work by Naghdi[3]. It allowed him to detect the onset of buckles and to predict their shape. I cannot speak with authority about the validity of the results because the mathematical methods are unfamiliar to me. However, it appears that his analysis, like Good and Straughan's, did not account for the boundary conditions at the entrance to the roller. In any event, it is a very interesting paper and illustrates the potential value of Naghdi's methods to web mechanics.

THE MODEL

As mentioned before, the curvatures in a thin twisted web will be quite small in relation to its flexural rigidity. And since the MD tension tends be large compared to all other stresses it can be safely assumed that the curvature in the machine direction will be virtually zero. This can be easily observed in a real web by holding the ends of a string against the web surface at the ends of a span. If the string is aligned with the machine direction it will be in full contact along its length, regardless of which surface of the web it is on. Thus, in the MD direction the web is neither concave nor convex. This is illustrated in Figure 1. This latex web is 5.5 inches wide and 0.030 mils thick. Tension is 3.7 pounds. A thread has been passed under the bottom roller and is draped over the top with a weight on its end. It is in full contact all along its length. The same thing will be observed if the string is on the opposite surface.

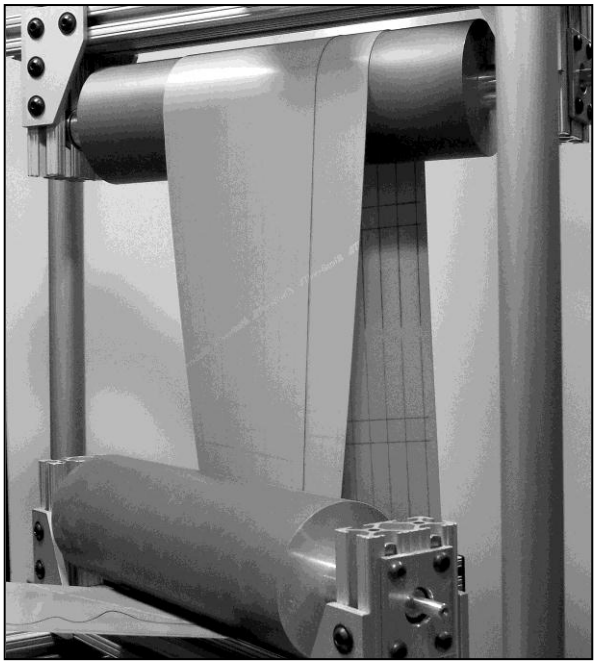

Figure 1 – Illustration of zero Curvature in the MD direction

One consequence of zero MD curvature is that curvature in the orthogonal direction will also be zero. This is easily observed by viewing twisted webs from the edge.

Zero MD curvature allows equation (3) in von Karman's model to be greatly simplified. It becomes simply,

$$\frac{\partial^2 w}{\partial x^2} = 0 \quad . \tag{4}$$

The next step in creating the model is to incorporate the features of finite deformation theory. Novoshilov[4] develops several versions of nonlinear theory that differ in complexity depending on the requirements. For problems with small strains and rotations the method described in Brown[5] is adequate. But, for large rotations it is

necessary to move up a step in complexity. In the following development, the strains are still considered to be small compared to unity. This permits the use of a formulation that is midway in complexity between those used in [5] and the general finite deformation equations.

Novoshilov's Small Strain, Large Rotation Equations

One of the greatest difficulties in working with this particular formulation of finite deformation theory is that one must think about the problem from the standpoint of two coordinate systems – the x-y-z coordinate system in which the problem is defined and another coordinate system which rotates with the deformation of the web surface. The essence of the method is to define the strains and stresses of the deformed body in terms of the undeformed coordinates, x and y. This makes it very easy to lose sight of the physical meaning of the quantities being calculated. For example, *u*, *v* and *w* are defined as displacements in the undeformed coordinates, x, y and z. Their derivatives relative to x and y are then used to define strains that apply to the deformed coordinates. So, it is always necessary to keep in mind whether a particular quantity is to be interpreted in terms of undeformed or deformed coordinates and to also define the direction cosines that permit transformation from one coordinate system to the other.

It should also be noted that the assumption of small strain makes it possible to assume that the deformed coordinate system remains orthogonal. Therefore, only rotations need be considered when transforming from one system to the other.

Strain definitions. These define the strains relative to the deformed coordinates.

Deformed x strain
$$\varepsilon_{xx} = \frac{\partial u}{\partial x} + \frac{1}{2}\left[\left(\frac{\partial u}{\partial x}\right)^2 + \left(\frac{\partial v}{\partial x}\right)^2 + \left(\frac{\partial w}{\partial x}\right)^2\right] \tag{5}$$

Deformed y strain
$$\varepsilon_{yy} = \frac{\partial v}{\partial y} + \frac{1}{2}\left[\left(\frac{\partial v}{\partial y}\right)^2 + \left(\frac{\partial u}{\partial y}\right)^2 + \left(\frac{\partial w}{\partial y}\right)^2\right] \tag{6}$$

Deformed shear
$$\varepsilon_{xy} = \frac{\partial u}{\partial y} + \frac{\partial v}{\partial x} + \frac{\partial u}{\partial x}\frac{\partial u}{\partial y} + \frac{\partial v}{\partial x}\frac{\partial v}{\partial y} + \frac{\partial w}{\partial x}\frac{\partial w}{\partial y} \tag{7}$$

Equilibrium equations. The stresses, σ_{xx} , σ_{yy} and σ_{xy} are referred to the deformed coordinate system. The terms within square brackets are the projections of these stresses onto the undeformed coordinates.

$$\frac{\partial}{\partial x}\left[\left(1+\frac{\partial u}{\partial x}\right)\sigma_{xx} + \frac{\partial u}{\partial y}\sigma_{xy}\right] + \frac{\partial}{\partial y}\left[\left(1+\frac{\partial u}{\partial x}\right)\sigma_{xy} + \frac{\partial u}{\partial y}\sigma_{y}\right] = 0 \tag{8}$$

$$\frac{\partial}{\partial x}\left[\left(1+\frac{\partial v}{\partial y}\right)\sigma_{xy} + \frac{\partial v}{\partial x}\sigma_{xx}\right] + \frac{\partial}{\partial y}\left[\left(1+\frac{\partial v}{\partial y}\right)\sigma_{yy} + \frac{\partial v}{\partial x}\sigma_{xy}\right] = 0 \tag{9}$$

$$\frac{\partial^2 w}{\partial x^2} = 0 \tag{10}$$

It might be less confusing if Novoshilov had used different subscripts for the stresses and strains that are referred to the deformed coordinate system. Since his work is so fundamental to this model, I've preserved his notation to avoid confusing those who may

want to refer to it. In defense of Novoshilov, however, he does go to some pains to explain the physical interpretation of his equations at many points throughout his book.

Throughout the remainder of this paper the subscripts x and y, when applied to the variables *u*, *v*, *w*, will indicate partial differentiation relative to that coordinate.

Direction cosines. Table 1 lists the cosines of the angles between the unit vectors of the deformed and undeformed coordinates.

	i_1 (deformed x)	i_2 (deformed y)
X	$\frac{1+u_x}{\sqrt{1+2\varepsilon_{xx}}}$	$\frac{u_y}{\sqrt{1+2\varepsilon_{yy}}}$
Y	$\frac{v_x}{\sqrt{1+2\varepsilon_{xx}}}$	$\frac{1+u_x}{\sqrt{1+2\varepsilon_{yy}}}$
Z	$\frac{w_x}{\sqrt{1+2\varepsilon_{xx}}}$	$\frac{w_y}{\sqrt{1+2\varepsilon_{yy}}}$

Table 1 – Direction cosines

The unit vectors i_1 and i_2 will be in the plane of the deformed web. Their direction will vary with x-y location. Coordinate i_3 will be orthogonal to the other two. It is not important to the analysis because a fundamental assumption in a two-dimensional model is that stresses perpendicular to the surface are zero.

Definitions of stress. These stresses are referred to the deformed coordinate system. For example, σ_{xx} is not the stress in the x direction. It is in the direction of a fiber in the deformed body that was parallel to the x-axis before deformation.

$$\sigma_{xx} = \frac{E}{1-\mu^2}\left(\varepsilon_{xx} + \mu\varepsilon_{yy}\right) \quad (11) \qquad \sigma_{yy} = \frac{E}{1-\mu^2}\left(\varepsilon_{yy} + \mu\varepsilon_{xx}\right) \quad (12) \qquad \tau_{xy} = \frac{E}{2(1+\mu)}\left(\varepsilon_{xy}\right) \quad (13)$$

Verification.

The mathematics was checked in the following way. Boundary conditions in the modeling software[1] were configured to rotate a stretched membrane about the x-axis without altering the stretching. The arrangement is shown in Figure 2 .

While in the horizontal position, the ends parallel with the y-axis are clamped in the y and z directions [$v = 0$, $w = 0$]. In the x direction, the clamped edges are fixed at one end [$u = 0$] and displaced at the other [$u = \Delta x$]. The edges parallel to x are left free. After running this case and collecting the results, a rigid body rotation was applied by changing the displacements in *v* and *w* at the clamped ends [$v = y \cdot cos(\theta) - y$ and $w = y \cdot sin(\theta)$]. Everything else was left the same. If the model works, the stress fields referred to the deformed coordinates should be the same. Results for σ_{xx} are shown in Figure 3. The membrane is ½ m by ½ meter by 0.1 mm thick, with a modulus of 10^9 Pa. The displacement, Δx is 1 mm.

[1] FlexPDE 5.0.15 from PDE Solutions, Sunol, CA

Figures 3 and 4 show identical stress fields as they should, because a rigid body rotation should not alter the stresses. The σ_{yy} stresses behave the same way.

The inverse cosine of $\frac{1+u_x}{\sqrt{1+2\varepsilon_{yy}}}$ in Figure 5 is within 0.13 percent of 30 degrees at all locations. This is also as it should be.

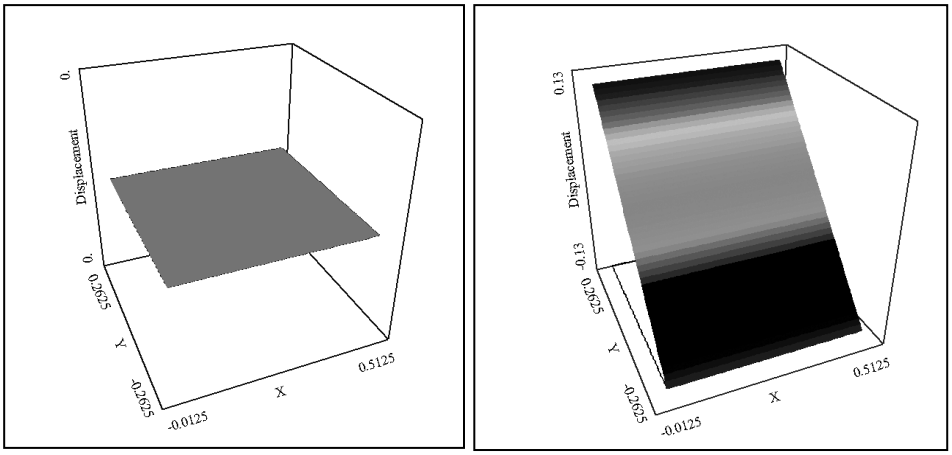

Figure 2 – Test Case

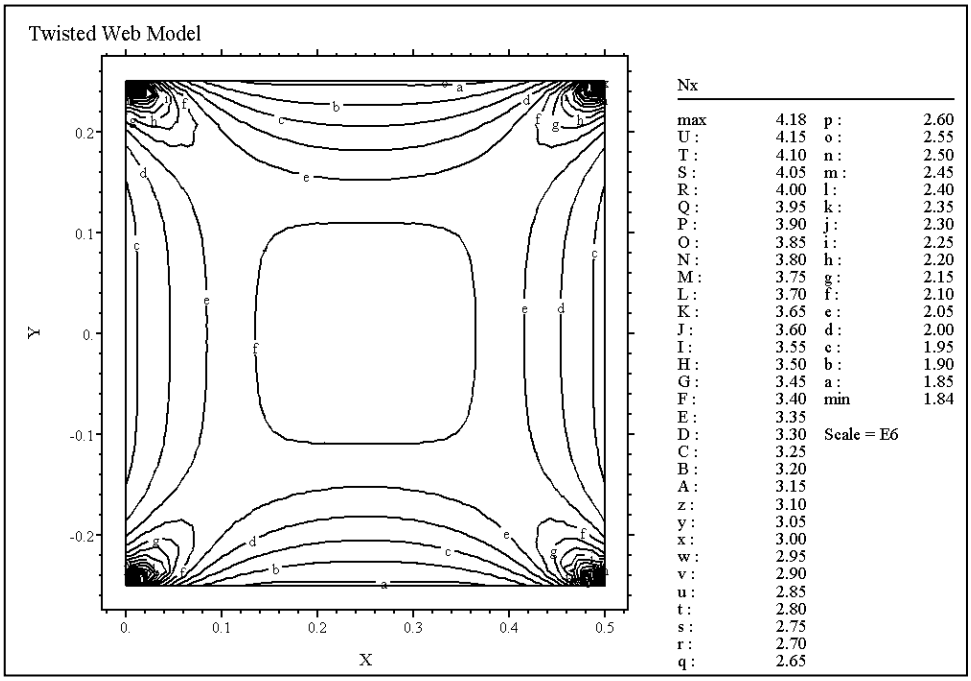

Figure 3 – Rotated 0 degrees

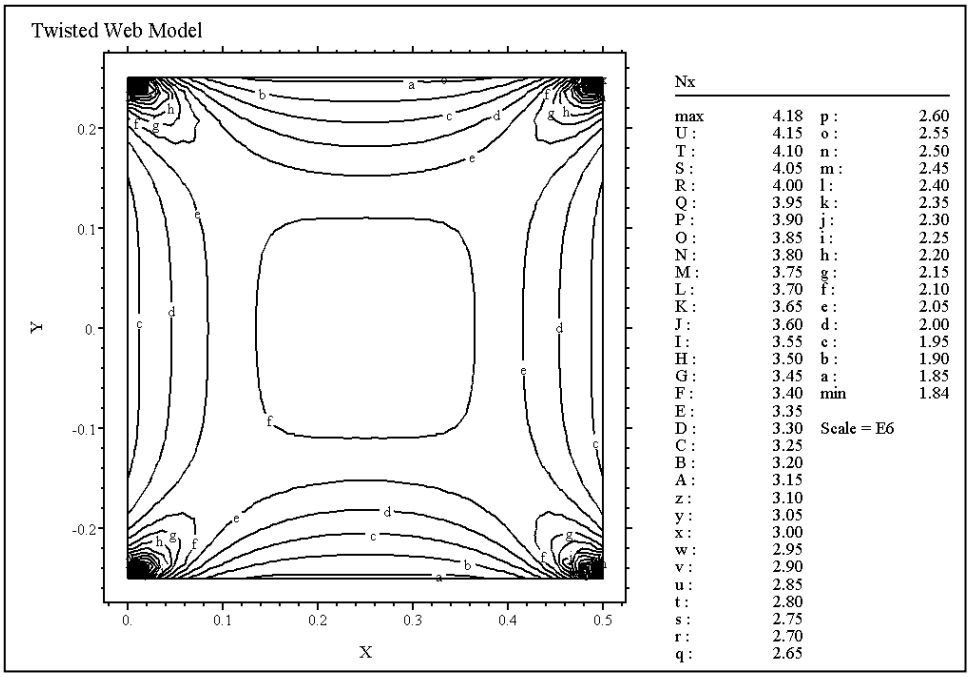

Figure 4 – Rotated 30 degrees

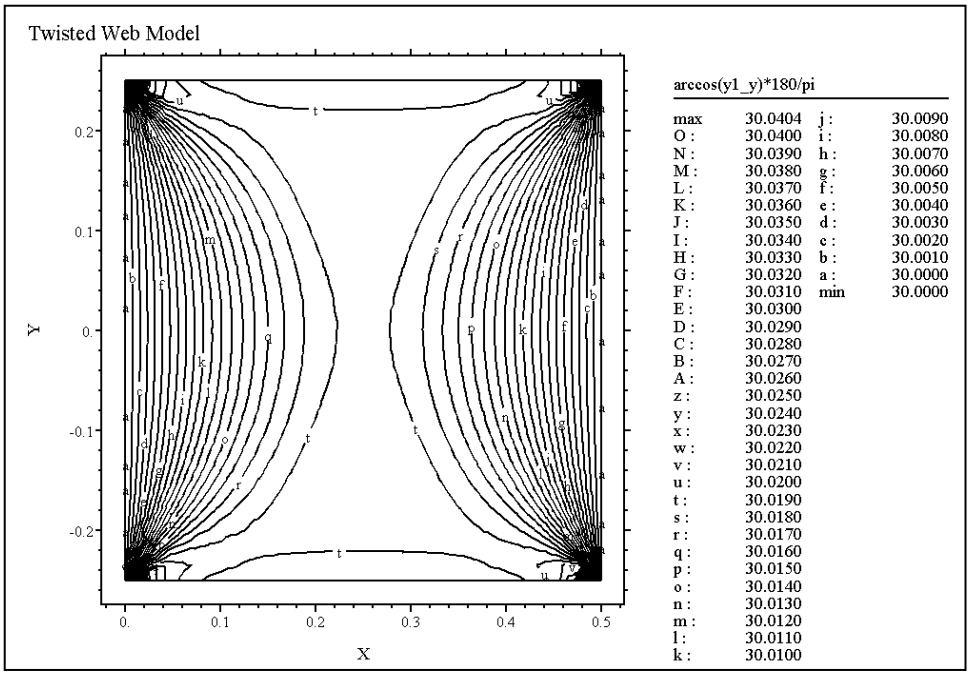

Figure 5 – The inverse cosine of $\frac{1+u_x}{\sqrt{1+2\varepsilon_{yy}}}$

Effect of Twist on Boundary Shape. As pointed out in [1], the roller boundaries of a twisted web are not parallel to the roller axes. Twist causes the wrap to increase at one edge and decrease at the other. Careful examination of Figure 1 shows this. Calculating the points of intersection of the web edges with the rollers is a straightforward, albeit tedious, exercise in numerical analysis. An iterative procedure was used for this work (available on request). There is also a slight CD curvature of the boundaries, due to the helical path they follow on the roller surfaces. This will generally be very small and will be ignored for purposes of this analysis.[2] The initial relaxed shape then becomes a parallelogram.

Boundary Defect. If a web running under tension could be stopped, frozen, cut along the line of entry at a roller and then unfrozen, the cut edge of the relaxed web would not match the original boundary. In the case of twisted webs, the effect is small. But, since an FEA solver makes the correction easy, it will be included. The problem is first solved with the relaxed boundary the same as the line of entry. Then, information from the solution is used to adjust the boundary to match the line of entry after deformation.

Spans Before and After the Twisted Span. This analysis will consider only a single span. To facilitate this, the previous span will be assumed to be in a state of pure MD stress. No attempt will be made to consider effects downstream of the span. Twisting a roller obviously twists both the upstream and downstream spans. So, eventually a two-span study must be made. But, one span is enough for now.

Boundaries. Figure 6 shows the general arrangement of boundaries and coordinates.

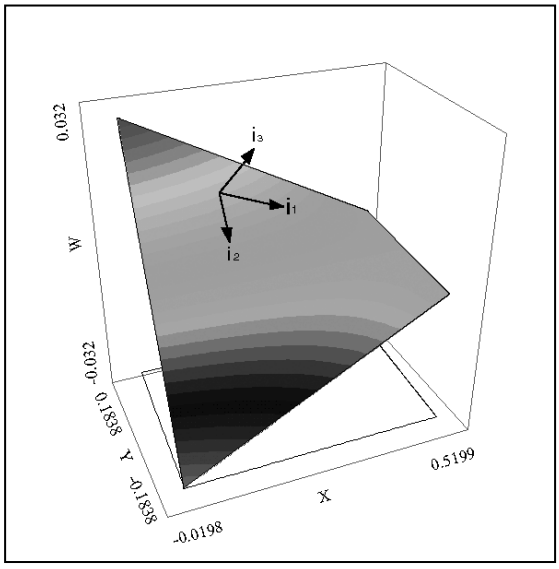

Figure 6 – Boundaries of the model

[2] This could be an important factor in more complex models that include wrinkling behavior because CD curvature at the boundaries may promote lateral instability in the presence of compressive stress.

All of the twisting is done at the upstream boundary. The downstream boundary is kept parallel to the *y*-axis with $w = 0$. This choice was made because the downstream boundary conditions are the most complicated and it seemed easier to avoid mistakes by keeping that boundary in the x-y plane. However, in a real world situation the circumstances would likely be reversed with the upstream end horizontal and the downstream end of the span rotated. This is an arbitrary choice, because it doesn't change the results, provided that all the previous spans are assumed to be in a state of pure MD stress and rotated (without twisting) into alignment with the upstream boundary.

At the upstream end, the *v* and *w* displacements will be used to twist the web through an angle, θ, while *u* is kept fixed.

Since there are three variables, *u*, *v* and *w*, three boundary conditions are required at each edge.

Lateral edge boundary conditions. The lateral edges are free of constraint. So, there will be zero normal stress and zero tangential shear. Therefore, the terms in the square brackets of the *y* derivative terms of (8) and (9) are set to zero.

$$\left(1+\frac{\partial u}{\partial x}\right)\sigma_{xy}+\frac{\partial u}{\partial y}\sigma_{y}=0 \qquad (14) \qquad \left(1+\frac{\partial v}{\partial y}\right)\sigma_{yy}+\frac{\partial v}{\partial x}\sigma_{xy}=0 \qquad (15)$$

There is no y derivative in (10). This implies that the y variation in *w* is completely determined by the x derivative in (10) and the conditions at the other boundaries. In other words, (10) and the boundary conditions on *w* at the rollers define a surface to which the membrane conforms. It is possible with FlexPDE to specify this requirement and allow it to solve for the surface.

Upstream boundary conditions. At the upstream roller, where the rotation will be established, it is necessary to specify all three boundary conditions in terms of displacements, *u*, *v*, and *w*. Displacement *u* is easy, it is fixed at zero. So,

Boundary condition 1 $$u=0 \quad . \qquad (16)$$

Displacements *v* and *w* require careful treatment because they are, by definition, referred to the undeformed coordinate system and yet they depend on the MD strain in the previous span (because it contracts in width), which is defined in terms of the deformed coordinate system. It will be assumed that the MD stress in the previous span is known to be equal to some value, σ_{xo}. Then the MD strain there will be $\varepsilon_{xo} = \sigma_{xo}/E$, and the CD strain will be $\varepsilon_{yo} = -\mu\varepsilon_{xo}$. In a linear elasticity analysis, the displacement *v* at the upstream boundary could now be calculated as $v = y\cdot(-\mu\varepsilon_{xo})$. This is not possible in the case of nonlinear analysis. The CD strain is defined by equation (6) . Therefore,

$$\frac{\partial v}{\partial y}+\frac{1}{2}\left[\left(\frac{\partial v}{\partial y}\right)^2+\left(\frac{\partial u}{\partial y}\right)^2+\left(\frac{\partial w}{\partial y}\right)^2\right]=-\mu\varepsilon_{xo} \qquad (17)$$

This is an ordinary differential equation that can be solved for *v*. It will be solved with the web in a horizontal position and then the rotation will be applied. The second term in the square brackets is zero because $u = 0$. The third term in the brackets is also zero because the web is in a horizontal position (zero slope along y). Therefore,

$$\frac{dv}{dy}=-1+\sqrt{1-2\mu\varepsilon_{xo}} \qquad (18)$$

Figure 6 illustrates how rotation affects *v*. From this it is apparent that,

Boundary condition 2 $$v = y\sqrt{1-2\mu\varepsilon_{xo}}\cos(\theta) - y \tag{19}$$

and

Boundary conditon 3 $$w = y\sqrt{1-2\mu\varepsilon_{xo}}\sin(\theta) \tag{20}$$

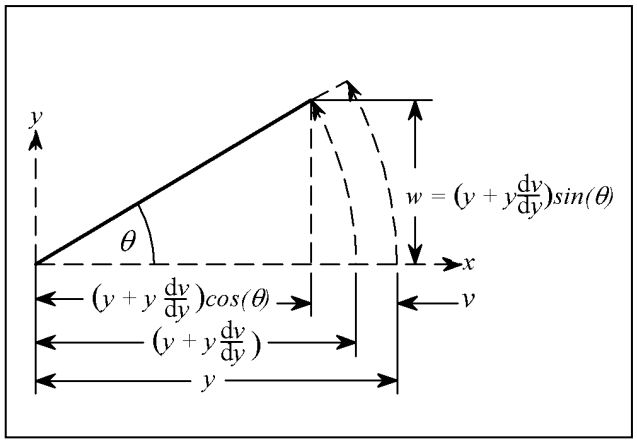

Figure 7 – Finding *v* and *w*

Downstream boundary conditions. At the downstream roller the z-axis displacement is zero. So,

Boundary condition 1 $$w = 0 \tag{21}$$

The normal strain and normal entry rules provide the other two conditions. The normal entry rule states that: *in a steady state, the path of a particle in the web aligns itself with the direction of the roller surface velocity (normal to the axis of the roller)*. In the undeformed state, the particle paths will be parallel to the x-axis. So, the vector defining the direction of the path in the deformed state is the direction of the unit vector for i_1. Since all the quantities in the calculation must be referred to the undeformed coordinate system, i_1 must be expressed in terms of the undeformed unit vectors, $\vec{x}$, $\vec{y}$. Using the direction cosines of Table 1, the vector $\vec{P}$ for the particle path will be,

$$\vec{P} = \frac{1+u_x}{1+E_x}\vec{x} + \frac{v_x}{1+E_x}\vec{y} \tag{22}$$

Therefore, the tangent of the entry angle, ψ, (which must become zero in the steady state) is,

Boundary condition 2 $$\tan(\psi) = \frac{v_x}{1+u_x} = 0 \tag{23}$$

Equation (23) is the second boundary condition for the downstream roller and is identical to the result found in reference 5, using a completely different approach.

The fact that the lines of contact with the rollers are not parallel with the roller axes has no effect on the application of the normal entry rule.

The normal strain rule states that*: in a steady state, the ratio of the stretched lengths of an infinitesimal patch of the web at two successive rollers is proportional to the respective ratios of the web velocities at the two rollers. In other words, if the web speeds up by 1% relative to the previous roller, it will have to elongate by 1% to insure that the mass flow is the same at the two locations.* Mathematically, this may be stated as,

$$\frac{1+\varepsilon_{xu}}{1+\varepsilon_{xd}} = \frac{V_u}{V_d} \tag{24}$$

Where ε_{xu} and ε_{xd} are the strains in the direction of the surface velocities of the rollers (normal to the axes of the rollers) and V_{xu} and V_{xd} are the respective velocities (also normal to the axes of the rollers). It is shown in reference 5 that the cross sectional area and density change by precisely the right amount to make this happen at each point across the web and that, furthermore, it must happen in order to satisfy the principle of conservation of mass. The requirement that the strains be the components normal to the roller axis is insured by the normal entry rule. Referring to Table 1, if v_x is zero then the angle between the deformed axis, i_1, and y must be 90 degrees.

Equation (24) makes it possible to define the strain, ε_{xx} at the downstream roller in terms of the strain at the entry to the upstream roller, ε_{xo} and the ratio of the circumferential velocities, V_u upstream and V_d downstream.

Boundary condition 3

$$\varepsilon_{xx} = \frac{V_u}{V_d}\left(1+\varepsilon_{xo}\right)-1 \tag{25}$$

Equation (25) is the third boundary condition for the downstream roller[3]. Since the strains are the values in the deformed web and are defined in terms of the undeformed coordinates, (25) needs no further transformation.

TYPICAL RESULTS

Typical results are illustrated for a PET web described in Good and Straughan's paper[1]. Test parameters are shown in the captions.

Figures 8 and 9 show contour plots of the principal stresses. The principal minimum stress (CD) in Figure 9 is compressive for almost the entire area of the span. [The principal angle relative to the x-axis varies from -4 to 4 degrees]. The principal maximum stress (MD) shows the expected parabolic profile, except near the roller where the normal entry and normal strain rules have must be satisfied.

Figures 10 and 11 show contour plots for the same PET web with a longer span. As the span lengthens, the CD compressive stress is localized at the roller, becoming zero in the middle section. The MD stress has a parabolic profile throughout its length. This is quite different than the flat web model. In the flat web, St. Venant's principle causes the MD profile to become uniform at cross sections that are not near the ends. Persistence of the profile in the FEA model is not an artifact of the analysis method. The topology of the 3D surface causes the MD strain profile to be distributed unchanged along the length.

---

[3] Equation (25) is different than the result presented in reference 5. In the earlier work an unnecessary approximation was used. It had no material effect on the results, because it produces nearly identical values for ε_{xx} . See Appendix A for an explanation.

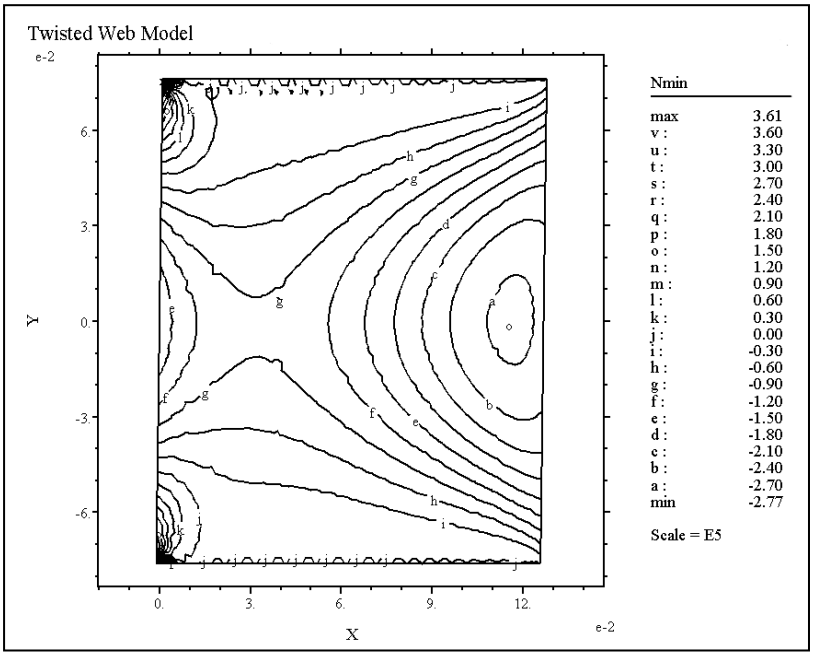

Figure 8 – Principal minimum stress (CD) PET web
Twist = 5 degrees. length = 0.108 m, width = 0.152 m, thickness = 23.4e-6 m, modulus = 4.13e9 Pa, tension = 26.7 N, μ = 0.3, roller diameter = 0.0736 m.

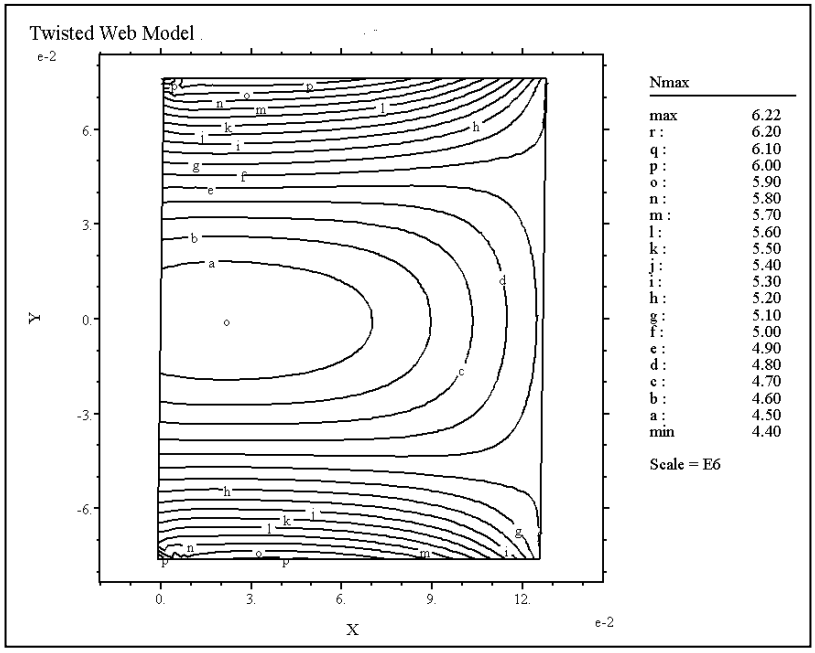

Figure 9 – Principal maximum stress (MD) – Same web as in Figure 8

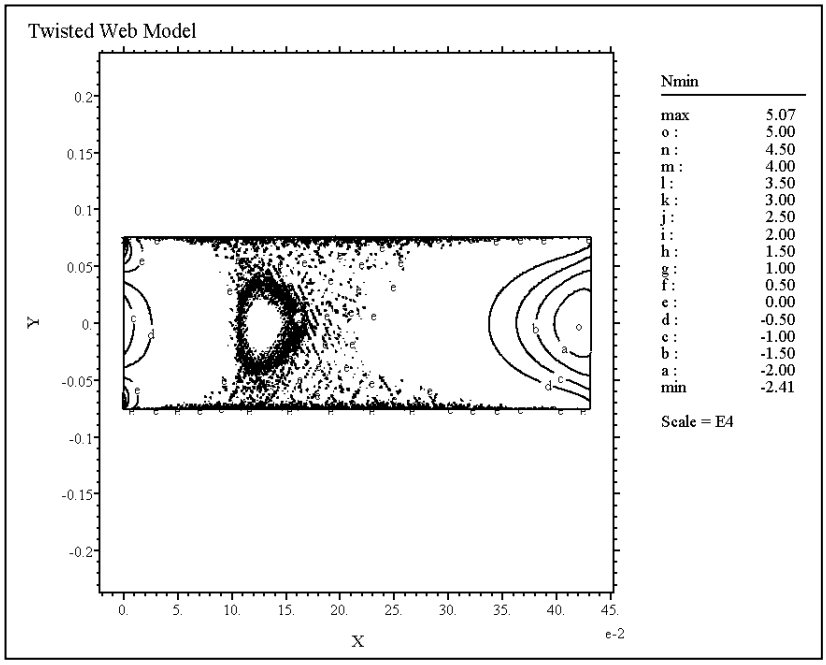

Figure 10 – CD Stress for **s**ame web as in figure 8 except L – 0.432 m

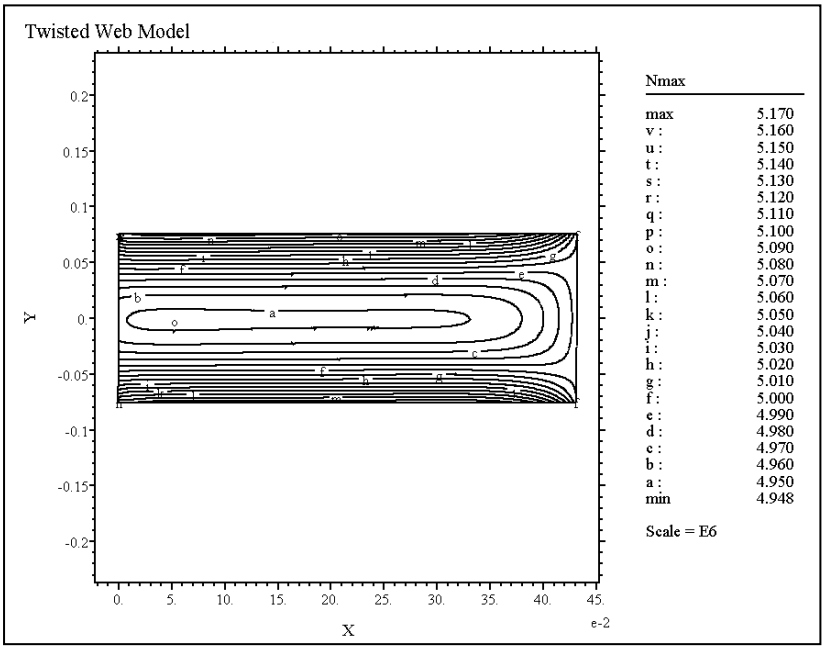

Figure 11 MD Stress – web same as figure 8 except L = 0.432 m

COMPARISON WITH AN EXPERIMENT.

Good and Straughan[1] performed a series of excellent experiments in which they increased the angle of twist until wrinkles occurred. The span length and tension were varied. In the paper they also developed a model based on the assumption that the stresses of a twisted web could be approximated in a flat web by applying an appropriately shaped MD stress profile to the ends. This was used in conjunction with Timoshenko's[6] critical stress, σ_{cr}, for buckling of a cylinder to predict the angle of wrinkling, ϕ_{cr}. In the following discussion, this will be called the G-S model. It will be interesting to compare the experimental data with the results of the G-S model the FEA model of the present paper.

The G-S model was organized to predict the angle of wrinkling, which was then compared with the observed angle. To facilitate inclusion of the FEA model in the comparison, the equations were rearranged to calculate the CD stress, σ_y, existing at the observed angle of wrinkling, ϕ_{cr}. The headings in the tables are: L = span length; σ_{xx} = Nominal MD stress; ϕ_{cr} = Observed angle of twist at which wrinkles appeared; σ_{cr} = Theoretical CD stress at which a cylinder will buckle; σ_{yA} = Theoretical CD stress from the G-S model; σ_{yF} = Theoretical CD stress from FEA model with the same inputs as the G-S model; σ_{yA}/σ_{yF} = Ratio of the G-S and FEA models CD stresses; ϕ_{cr}/L = Ratio of the observed critical angle of twist to the span length. All of the CD stresses were peak values at the roller.

The last entry in Table 3 is a calculation to check the rearranged math. Unlike the other rows, the angle used for ϕ_{cr} was the value predicted by the G-S model rather than the observed value. This resulted in σ_{yG} being equal to σ_{cr} as it should have.

	L (m)	σ_{xx} (Mpa)	ϕ_{cr} (Deg.)	σ_{cr} (Mpa)	σ_{yG} G-S Flat (Mpa)	σ_{yF} FEA Twisted (Mpa)	σ_{yG}/σ_{yF}	ϕ_{cr}/L (Deg./m)
1	0.108	15	4.1	-1.59	-1.85	-0.86	2.2	38
2	0.108	30	4.6	-1.59	-2.33	-1.1	2.1	43
3	0.464	15	10	-1.59	-2.0	-0.27	7.4	22
4	0.464	30	9.8	-1.59	-1.92	-0.27	7.0	21

Table 2 - PET
Width = 0.152 m, thickness = 23.4e-6 m, modulus = 4.13e9 Pa, $\mu = 0.3$,
roller diameter = 0.0736 m, uncoated aluminum surface

	L (m)	σ_{xx} (Mpa)	ϕ_{cr} (Deg.)	σ_{cr} (Mpa)	σ_{yG} G-S Flat (Mpa)	σ_{yF} FEA Twisted (Mpa)	σ_{yG}/σ_{yF}	ϕ_{cr}/L (Deg/m)
5	0.127	5	2.7	-1.21	-0.76	-0.28	2.7	21.3
6	0.127	15	3.0	-1.21	-0.94	-0.35	2.7	23.6
7	0.127	25	3.0	-1.21	-0.94	-0.35	2.7	23.6
8	0.432	5	7.4	-1.21	-1.29	-0.18	7.2	17.3
9	0.432	15	8.8	-1.21	-1.82	-0.26	7.0	20.4
10	0.432	25	9.0	-1.21	-1.90	-0.28	6.8	20.8
11	0.584	5	10.8	-1.21	-1.28	-0.21	6.1	18.5
12	0.584	15	11.8	-1.21	-1.53	-0.25	6.1	20.2
13	0.584	25	12	-1.21	-1.59	-0.27	5.9	20.5
	0.584	5	10.5	-1.21	-1.21			

Table 3 – PET
Width = 0.152 m, thickness = 17.8e-6 m, modulus = 4.13e9 Pa, μ = 0.3,
roller diameter = 0.0736 m, high friction coating on roller

	L (m)	σ_{xx} (Mpa)	ϕ_{cr} (Deg.)	σ_{cr} (Mpa)	σ_{yG} G-S Flat (Mpa)	σ_{yF} FEA Twisted (Mpa)	σ_{yG}/σ_{yF}	ϕ_{cr}/L (Deg./m)
14	0.127	13	1.7	-0.96	-0.65	-0.22	3.0	13.5
15	0.127	26	2.1	-0.96	-0.99	-0.25	4.0	16.5
16	0.127	40	2.7	-0.96	-1.63	-0.58	2.8	20.5
17	0.584	13	6.5	-0.96	-1.00	-0.16	6.3	11.1
18	0.584	26	7.8	-0.96	-1.44	-0.23	6.3	13.4
19	0.584	40	7.9	-0.96	-1.48	-0.24	6.2	13.5

Table 4– PEN
Width = 0.152 m, thickness = 6.6e-6 m, modulus = 8.87e9 Pa, μ = 0.3,
roller diameter = 0.0736 m, high friction coating on roller

	L (m)	σ_{xx} (Mpa)	ϕ_{cr} (Deg.)	σ_{cr} (Mpa)	σ_{yG} G-S Flat (Mpa)	σ_{yF} FEA Twisted (Mpa)	σ_{yG}/σ_{yF}	ϕ_{cr}/L (Deg./m)
20	0.127	3.9	3.5	-0.28	-0.11	-0.036	3.1	27.6
21	0.127	13.1	5.0	-0.28	-0.21	-0.076	2.8	39.4
22	0.584	3.9	13.5	-0.28	-0.17	-0.025	6.8	19.7
23	0.584	13.1	15.0	-0.28	-0.20	-0.032	6.3	22.4

Table 5 – Polyethylene
Width = 0.152 m, thickness = 50.8e-6 m, modulus = 0.34e9 Pa, μ = 0.3,
roller diameter = 0.0736 m, high friction coating on roller

CONCLUSIONS.

1. The FEA model shows significantly lower levels of CD compressive stress at the critical angle than the G-S model. They are 1/3 to 1/7 as large.
2. With the exceptions of tests 1, 2 and 16, the FEA model produced CD stresses that varied less with tension and span length.
3. The ratio of the stress magnitudes between two models changes with span length. For a given length, the ratio is approximately the same across all the tests. This may be due to the difference in the behavior of the MD stress profiles in the two models. The FEA model tends to have a parabolic stress profile throughout its length whereas the G-S model does not. The difference becomes more significant for long spans.
4. If the FEA model is more accurate in predicting the CD stress, then a new buckling criterion must be developed. Something along the lines of the criterion used by Good, Kedl and Shelton[7] for shear wrinkling may be appropriate.
5. Both models show very little change in CD stress levels with tension.
6. Until someone solves the problem of measuring stress levels in thin webs, the wrinkling threshold will probably remain the best validity test for twisted web models.
7. There is nothing in the FEA modeling technique to detect CD elastic instability. More work should be done to incorporate the features of the von Karman equations.

It should be emphasized that the G-S model is still the best tool available for predicting the onset of wrinkling with twist. It may overestimate the magnitude of the CD stress. But if that is the case, the buckling criterion must be doing the same thing because the results agree well with experiment.

A Hypothesis to explain CD compressive stress with twist

Both the experiments and the models indicate that the compressive stress doesn't change much with the MD tension? One likely explanation is that the compressive CD stress is primarily due to the effect of the normal entry rule at the roller.

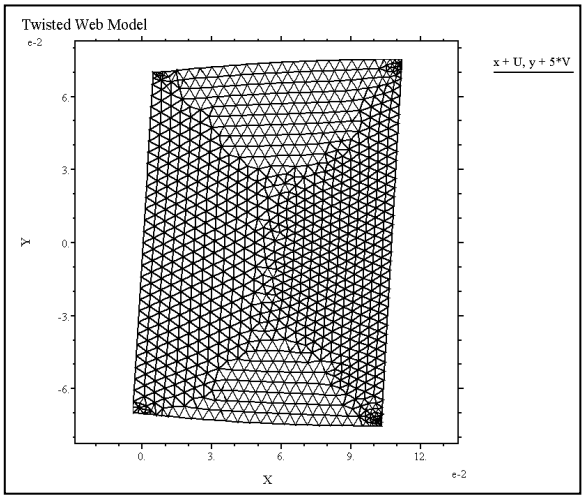

Figure 12 – **Projection of deformed boundaries on x-y plane**

Figure 12 shows the shape of the deformed web projected on the x-y plane. The twist has been increased to 10 degrees and the y displacement scaled up so that the shape is easier to see. The upstream twist has caused the particle paths to become curved in the vicinity of the downstream boundary. Keep in mind that the downstream boundary is in the x-y plane. So, there is "real" curvature there. The curvature causes the normal entry rule to create the lateral compression (the slanted web boundary caused by its parallelogram shape has nothing to do with this). If traction permits, the web is compressed laterally until the particle paths are bent into alignment with the velocity vector of the roller surface.

To check this hypothesis, the model was modified at the downstream boundary to eliminate the normal entry condition in two different ways. First, a boundary condition for displacement *v* was applied, matching that at the upstream roller. Displacement, *w* was zero as before. Displacement *u* was chosen to create a uniform MD tension prior to twisting. So, the model was equivalent to a web running under tension between parallel rollers that is then stopped and twisted. Under these conditions additional MD stress produced by the twisting causes the web to neck down at the roller, producing tensile CD stress. Next, the model was changed so that there would be no axial traction at the downstream roller – a free edge in the y direction. The other boundary conditions were the same as the first case. There was compressive CD stress at the roller. But, it was an order of magnitude smaller than with the normal entry condition active

Slipping

In almost all of the tests described in [1] the critical angle of twist did not change significantly with tension. There were some cases where this was not true.

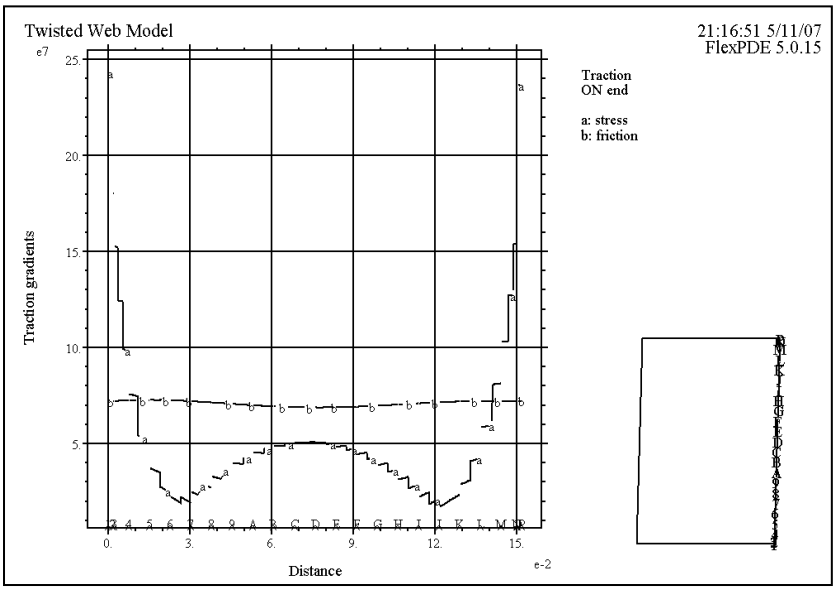

Figure 13 – Friction and stress rates at 26.7 N
Twist = 5 degrees. length = 0.108 m, width = 0.152 m, thickness = 23.4e-6 m, modulus = 4.13e9 Pa, tension = 26.7 N, $\mu = 0.3$, roller diameter = 0.0736 m.

If the tension was low, it sometimes took much more twist (as much as two times) to create a wrinkle than at higher tensions. In a graph with critical twist angle on the ordinate and tension on the abscissa, the twist angle would start high and then become asymptotic to a horizontal line as the tension increased. The authors suggested that low friction between the web and roller might have allowed troughs to flatten at the roller. This conclusion is supported by Figure 13, which shows a plot of the magnitude of the stress and friction rates at each point across the web.

The values in Figure 13 were computed as part of the FEA analysis, based on unpublished work by the author. The stress rate (rate in terms of distance, Pa/m) is the combined effect of the axial and circumferential stresses that are available to overcome friction. The friction rate is the maximum value of the radial stress (normal to the web surface) times the coefficient of friction divided by the radius of curvature of the roller surface. [The direction of the maximum friction rate is not necessarily circumferential. So, the radius of curvature is usually larger than the cylinder radius.] At any location where the stress rate is larger than the friction rate, local slipping may occur. The friction rate in Figure 12 is based on a friction coefficient of 0.3. It is evident that the edges can slip and that it would take only a slight change in either coefficient or stress for any of the other points to slip. In all of the other cases where this behavior was observed, the FEA analysis produced data like Figure 13 or worse (with the friction curve below the stress curve). In all other cases where "normal" behavior was observed there was ample separation between the stress and friction rate curves.

APPENDIX A

Alternative Derivation of Normal Strain Rule
And an Unnecessary Approximation

In the diagram below, the web is assumed to be running in a steady state with good traction on the rollers.

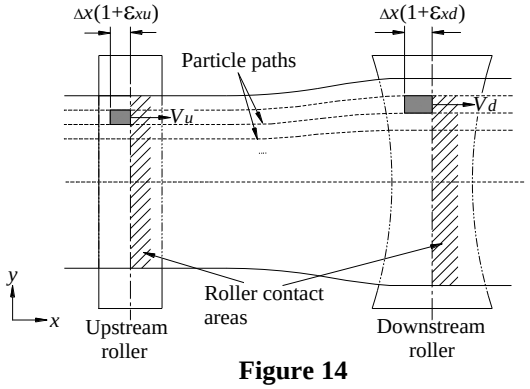

Figure 14

At the entry to the rollers, the normal entry rule requires that the particle paths be normal to the axis of rotation of a roller surface. The shaded area at the entry to the upstream roller represents an infinitesimal area with sides parallel to two particle paths. The shaded area at the entry to the downstream roller is the same portion of web at the moment that it enters the roller there. The roller surface velocities are V_u and V_d. Δx is the relaxed length of the area in direction x. ε_{xu} is the strain normal to the upstream roller. ε_{xd} is the strain normal to the downstream roller. Conservation of mass requires that the mass flow into and out of the span for any portion of web between two particle paths be

constant. Otherwise, material would accumulate in the span and a steady state would not exist. For this to be true, each area must travel past the line of roller contact in the same length of time. Therefore,

$$\Delta x\left(1+\varepsilon_{xu}\right)=V_u\,\Delta t \tag{26}$$

and

$$\Delta x\left(1+\varepsilon_{xd}\right)=V_d\,\Delta t \tag{27}$$

Equating (26) and (27) and solving for ε_{xd}

$$\varepsilon_{xd}=\frac{V_d}{V_u}\left(1+\varepsilon_{xu}\right)-1 \tag{28}$$

Equation (28) is not the same as that developed in "A New Method for Analyzing the Deformation and Lateral Translation of a Moving Web"[5]. However, the two equations are numerically equivalent for small strains. In the method of derivation used in [5], separate expressions were developed for the mass flows at the upstream and downstream rollers. For example, the mass flow upstream is,

$$Q_i=\frac{V_u\,(dy)(h)(\rho_o)}{\left(1+\varepsilon_{xu}\right)} \tag{29}$$

where *dy* is the increment of width, *h* is the thickness and ρ_o is relaxed density. The strain in the denominator looked like a potential nonlinearity. So, the approximation,

$$\left(1+\varepsilon_{xu}\right)^{-1}\approx\left(1-\varepsilon_{xu}\right) \tag{30}$$

was used. This led to the relationship,

$$\varepsilon_{xd}\approx 1-\frac{V_u}{V_d}\left(1-\varepsilon_{xu}\right) \tag{31}$$

.

Although (31) is algebraically different than (28), the numerical difference in ε_{xd} is insignificant so long as ε_{xu} is very small and *Vu/Vd* is close to 1. Both of these requirements are met in any practical web handling problem. Note that when *Vu/Vd* =1 they are exactly equivalent and that was the value assumed for all the examples in the paper. Nevertheless, the concern about a nonlinearity was misguided. Leaving (29) alone, along with its companion expression downstream, would have led to (28) which is exact and linear.

---

1. Good, J. K. , Straughan, P., "Wrinkling of Webs Due to Twist," Proceedings of the Fifth International Conference on Web Handling, June 1999, pp 509-523

2. Mockensturm, E. M., "The Elastic Stability of Twisted Plates," Journal of Applied Mechanics, July 2001, Vol 68, pp 561-567

3. Naghdi, P. M., "The Theory of Shells and Plates," S. Flugge's Handbuch der Physik, Vol VIa/2, C. Truesdell, ed., Springer-Verlag, Berlin, pp 425-633

4. Novoshilov, V. V., Foundations of the Nonlinear Theory of Elasticity, Graylock, 1953

5. Brown, J. L., "A New Method for Analyzing the Deformation and Lateral Deformation of a Moving Web," Proceedings of the Eighth International Conference on Web Handling, pp 39-59

6. Timoshenko, S.P., "Theory of Elastic Stability," McGraw-Hill, 1936, pp 467-470

7. Good, J. K., Kedl, D. M., Shelton, J. J., "Shear Wrinkling in Isolated Spans," Proceedings of the Fourth International Conference on Web Handling, pp 462-471